3 J/1 Hz opposite diode-pumped Yb:YAG active mirror amplifier at room temperature

Jinsheng Liu [1], Lailin Ji [1,*], Yukun Zhu [1], Xianghe Guan [1], Jiaqi Zhang [1], Jingzhe Yang [1], Jiangnan Chu [1], Tao Wang [1], Wei Feng [1], Lan Xia [1], Dong Liu [1], Ruijing He [1], Tianxiong Zhang [1], Yong Cui [1], Zhan Sui [1], Xiaohui Zhao [1], Yuqiu Gu [1] and Yanqi Gao [1]

[1] *Shanghai Institute of Laser Plasma, China Academy of Engineering Physics, Shanghai 201800, China*

Abstract Experimental amplification of 10-ns pulses to an energy of 3 J at a repetition rate of 1 Hz is reported from an opposite diode-pumped Yb:YAG-based active mirror amplifier at room temperature. Meanwhile, we have conducted the crystal packaging, amplified spontaneous emission (ASE) suppression, coating design, and pump energy storage. The gain characteristics dependence on pump pulse duration, cooling-water temperature, and repetition rate are studied. The compact amplifier employs symmetrically placed active mirror amplifiers, with a 2-m optical length and a footprint of 60×80 cm^2. Thanks to Gaussian spatial profile of the beam, no telescope was required in the entire amplifier chain. The validated concept of the compact active mirror amplifier shows potential for scaling energy up to 50 J or beyond by incorporating additional active mirrors into the chain, especially seeding with a pulse energy of ×100-mJ at repetition rate of 1-10 Hz.

Key words: Solid-state laser; High energy laser; Active mirror amplifier; Repetition rate laser.

Correspondence to: Lailin Ji, Shanghai Institute of Laser Plasma, China Academy of Engineering Physics, Shanghai 201800, China. Email: jsycjll@siom.ac.cn

This peer-reviewed article has been accepted for publication but not yet copyedited or typeset, and so may be subject to change during the production process. The article is considered published and may be cited using its DOI.

This is an Open Access article, distributed under the terms of the Creative Commons Attribution licence (https://creativecommons.org/licenses/by/4.0/), which permits unrestricted re-use, distribution, and reproduction in any medium, provided the original work is properly cited.

10.1017/hpl.2026.10219

Downloaded from https://www.cambridge.org/core. 17 Nov 2026 at 18:24:11, subject to the Cambridge Core terms of use.

I. Introduction

Yb:YAG has attracted considerable research interest due to its outstanding optical properties, enabled by the continuous advancement of laser diode (LD). Its absorption wavelength is closer to the emission wavelength, resulting in a low quantum defect of ~9% [1-2]. The fluorescence lifetime of Yb:YAG (950 μs) is about four times longer than that of Nd:YAG (230 μs), beneficial for efficient storage of pump energy [3]. Yb^{3+} ions exhibit superior compatibility with the YAG matrix, which allows for high doping concentrations [4]. Even at elevated doping levels, the medium remains free from several loss mechanisms, including excited-state absorption, concentration quenching and upconversion [5]. Additionally, Yb:YAG possesses high thermal conductivity [6-7]. These favorable properties make Yb:YAG a widely adopted gain medium for high-energy solid-state lasers with repetition rate [8-10].

Table 1 summarizes the research progress on tabletop room-temperature Yb:YAG lasers delivering hundreds of millijoules pulses [11-21]. Regenerative amplifier followed by traveling-wave amplifier represents an effective approach for Yb:YAG to achieve an energy of ×100 mJ. However, this compact combination offers limited advantages for the development of high-energy outputs, with the current maximum output achieving only 1 J/2 Hz/4 ns [15]. One notable exception is LUCIA, which reaches an output of 14 J/2 Hz/10 ns [22-25]. Nevertheless, its ~10 m^2 footprint and the requirement for cryogenic operation (100-200 K) of the second amplifier constrain practical application scenarios. Despite well-known advantages of thin-disk lasers in high average power output, the intrinsic geometric configuration imposes inherent limitations on boosting energy up to Joule-level: (1) The use of a sub-millimeter-thick gain medium to realize a one-dimensional thermal gradient and almost eliminate thermal lens effect, directly restricts the energy storage volume. (2) The extremely large diameter-thickness ratio (>100) of the disk renders it highly susceptible to ASE in transverse direction. The transverse gain-length product can readily exceed 4, leading to a rapid depletion of upper-level population and a severe reduction in energy storage capacity. These two coupled physical constraints render the thin-disk architecture

Downloaded from https://www.cambridge.org/core. 17 Nov 2026 at 18:24:11, subject to the Cambridge Core terms of use.

unsuitable for generating pulses with energies of Joule-scale or even up to ×10 J. To overcome the energy limitations while preserving the benefits of diode-pumping, a laser amplifier employing a bulk gain medium becomes essential.

Table 1. Research progress on hundred millijoule pulses based on Yb:YAG at room temperature.

Year	Output energy (mJ)	Repetition rate (Hz)	Pulse duration (ps)	Optical-to-optical efficiency	Ref.
2008	220	10	6400	10%	[11]
2009	400	100	2.0	14%	[12]
2011	200	10	0.9	4%	[13]
2012	100	1000	1.6	12%	[14]
2014	1000	2	4000	7%	[15]
2015	220	1000	1.9	28%	[16]
2016	306	100	1.8	18%	[17]
2016	600	100	2.0	9%	[18]
2017	200	5000	1.1	7%	[19]
2020	720	1000	0.9	8%	[20]
2024	110	1000	2.1	11%	[21]

Our research lies in the development of compact Yb^{3+}-doped laser amplifiers operating at room temperature. In our previous works, an amplifier design based on two symmetrically placed active mirrors was introduced. We subsequently developed a spatial displacement-angle encoding architecture which integrates multi-pass amplification into the same gain medium, enabling a tabletop 20-TW optical system [26-27]. In this active mirror configuration, one large face of the slab-shaped gain medium serves as a reflective mirror, and the laser beam follows a V-shaped path to extract the stored energy. The same reflective surface also functions as the pump and cooling interface for the gain medium. Careful encapsulate of the active mirror is required to preserve its surface flatness while ensuring efficient convective heat transfer.

In this work, we experimentally demonstrate a room-temperature active mirror amplifier based on Yb:YAG. Key aspects of the compact amplifier design, including crystal packaging, ASE suppression, coating design, and pump energy storage are addressed. The gain characteristics are investigated under various operating conditions. A double-stage active mirror amplifier scheme is proposed, delivering a 3 J/1 Hz/10 ns pulse from an injection energy of 300 mJ. These results highlight the capability of the opposite diode-pumped Yb:YAG-based amplifier for generating Joule-level pulses at room temperature.

Downloaded from https://www.cambridge.org/core. 17 Nov 2026 at 18:24:11, subject to the Cambridge Core terms of use.

II. Basic characteristics of active mirror amplifier

2.1 Design and packaging of active mirror amplifier

Figure 1 presents a three-dimensional view of the active mirror amplifier. Yb:YAG crystal was selected as the gain medium for the compact repetition-rate active mirror laser amplifier. Considering the product of doping concentration and thickness, the diameter-to-thickness ratio, and the gain-length product, we have designed the gain medium with dimensions (*xyz*) of $60\times35\times6$ mm^3 (Figure 1) and a doping concentration of 2 at. %. To minimize the impact of cooling water on pulse wavefront and enhance the cooling efficiency, we have adopted an opposite pumping configuration, as illustrated in Figure 1(a), where the pump and signal beams are incident on opposite sides of the gain medium. Water was chosen as the coolant due to its high heat capacity, excellent fluidity, easy availability, and cost-effectiveness, making it well suited for high-energy solid-state lasers. We deionize the water and incorporate silver wires to suppress microbial growth.

The primary advantages of this configuration are as follows: (1) It decouples the cooling flow channel from the pulse optical path, thus preventing flow-induced turbulence from perturbing the laser pulse wavefront and degrading the output beam quality; (2) It allows direct contact between the coolant and the hottest surface of the gain medium, ensuring efficient convective heat transfer and consequently achieving high cooling efficiency; (3) It establishes a thermal gradient approximately along with *z* (Figure 1(a)), thereby minimizing the impact of heat generation within the crystal on the amplified beam quality. An ingenious coating design was tailored for our room-temperature amplifier, enabling seed amplification and pump energy storage within a waterproof configuration, as illustrated in Figure 1(a). The glass serves to encapsulate the cooling water, and Surface 1 need to maintain high transmittance for pump. Therefore, Surface 1 was coated with an anti-reflective film at the pump wavelength. Surface 2 can remain uncoated as the refractive index of glass (~1.44) closely matches that of the cooling water (~1.33). According to the Fresnel equations, the resulting interface reflectance is less than 0.5%, rending an anti-reflective coating unnecessary. Surface 3 functions as both the transmission surface for the pump and the reflective surface for the signal. Therefore, while ensuring the waterproofing of coating, it must exhibit high

Downloaded from https://www.cambridge.org/core. 17 Nov 2026 at 18:24:11, subject to the Cambridge Core terms of use.

transmittance for the pump and high reflectance at the signal wavelength. To meet compact design of the amplifier, the two gain media are positioned directly opposite each other, which introduces a risk of parasitic optical cavity. Hence, surface 3 requires an anti-reflective treatment for signal incident at shallow angles (~0°). This measure is crucial for achieving a compact system layout, while simultaneously maintaining amplification capability and suppressing ASE. The coating design for surface 4 is comparatively straightforward, requiring high reflectance for pump and high transmittance for the signal incident at the Brewster angle.

The designed coating enables twice absorption of pump (shown in Figure 1(b)), minimizes surface reflection losses of signal, and effectively enhances the overall amplifier performance. A tilted pumping scheme is adopted, whereby the residual pump source after twice absorption is captured by an optical dump, effectively preventing any potential damage to the LD. To suppress ASE and parasitic oscillation effects within the gain medium, we employ a Cr:YAG crystal as the cladding medium, with an absorption coefficient of 4 cm^{-1} at 1030 nm and a single-sided cladding thickness of 8 mm along both *x*- and *y*- axes (Figure 1(c)). The use of identical host materials minimizes the refractive index mismatch at the interface, thereby improving energy storage in the gain medium.

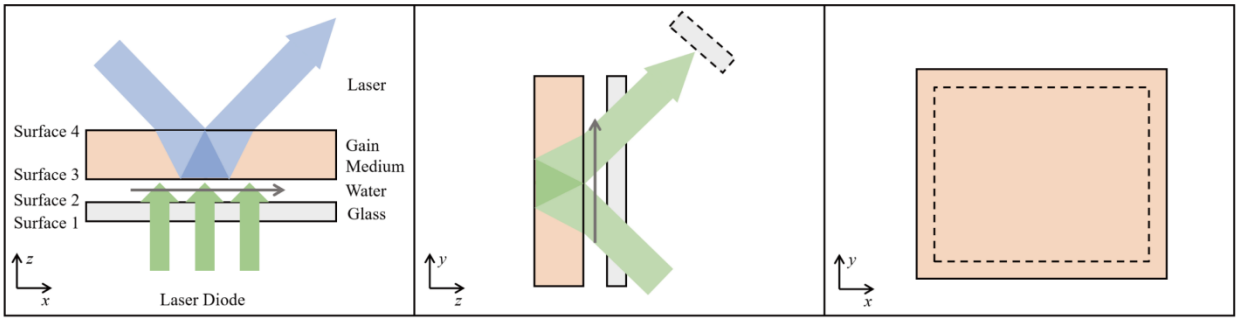


Figure 1. Schematic diagrams of active mirror amplifier, with (a), (b), and (c) showing the *xz*, *yz*, and *xy* planes, respectively. (a) Surfaces 1, 2, 3, and 4 denote the interfaces between air and glass, glass and cooling water, cooling water and gain medium, as well as gain medium and air. A high-quality glass with dimensions (*xyz*) of 76×51×3 mm^3 is employed. The cooling water, with a thickness of 3 mm, flows at a rate of 15 L/min. (b) The tilted pump beam undergoes twice absorption by the gain medium. With an additional reflective mirror, the absorption by the gain medium occurs four times. (c) The gain medium measures 60×35×6 mm^3 in size, featuring a doping concentration of 2 at. %. All four lateral sides (length and width) are clad with an 8-mm-

Downloaded from https://www.cambridge.org/core. 17 Nov 2026 at 18:24:11, subject to the Cambridge Core terms of use.

thick layer of undoped YAG.

2.2 Pump source architecture

To guarantee the output performance of amplifier while minimizing the volume and weight of the pump source, we have developed a compact pumping scheme with a high-intensity LD. In this configuration, Surface 1 (Figure 1(a)) of glass is closely attached to the pump. Both LD arrays consist of 8 stacks and each stack contains 32 bars, with each bar delivering an output power of 420 W. After collimation and homogenization, the output power of LD source is approximately 100 kW. We characterized the central wavelength of the LD output under various repetition rate (Figure 2(a)) and cooling-water temperature (Figure 2(b)). (Note: Only the LD cooling water temperature is varied, while the crystal temperature is fixed at 293.15 K via two separate water cooling circuits. The reason for selecting 293.15 K as the working temperature for the crystal is as follows: (a) The variations in both emission cross-section and emission bandwidth of Yb:YAG within the temperature range of 288.15-298.15 K are considered negligible. (b) The laboratory temperature is maintained at 298.15 K. Employing higher temperatures would be equivalent to heating the crystal, leading to unnecessary energy consumption. (c) When the crystal operates at temperatures below 288.15 K, surface condensation occurs, affecting the performance of amplifier.) At a temperature of 292.15 K, the central wavelength increased from 927.0 nm to 936.2 nm as the repetition rate was raised from 1 Hz to 20 Hz. Similarly, with the repetition rate fixed at 1 Hz, the central wavelength shifted from 927.0 nm to 935.8 nm as the cooling-water temperature increased from 292.15 K to 318.15 K. The emission wavelength of LD in both cases exhibits a redshift, originating from essentially the same physical mechanism: the rise in junction temperature, which is the actual temperature within the active region of the chip. An increase in junction temperature directly reduces in the bandgap energy (Eg) of the semiconductor material. According to the relation λ (nm) $\approx$ 1240 (eV·nm) / Eg (eV), a decrease in bandgap directly translates to a longer emission wavelength. This phenomenon is primarily attributed to lattice thermal expansion. The typical magnitude of redshift in LD emission wavelength ranges from +0.3 nm/K to +0.4 nm/K. It should be emphasized that the emission wavelength is a consequence, rather than the cause, of the junction temperature. When all other conditions remain the same, a lower

Downloaded from https://www.cambridge.org/core. 17 Nov 2026 at 18:24:11, subject to the Cambridge Core terms of use.

junction temperature results in a shorter emission wavelength and effectively extends the operational lifetime.

The spectral profile of the LD output at 1 Hz and 318.15 K is shown in Figure 2(c), featuring a central wavelength of 935.8 nm and a full width at half maximum (FWHM) of 4.9 nm. The emission spectrum of the LD (Figure 2(c)) and the absorption spectrum of a 2 at. % doped Yb:YAG crystal were considered in the calculations. The simulation yields a twice-absorption curve of pump with a pump absorption rate of 89.8%, as illustrated by the cyan solid line in Figure 2(d). The multi-pass absorption design guarantees sufficient energy storage even with a slightly lower initial wavelength. To further enhance the pump intensity, we proposed a pumping scheme utilizing titled pumping with four-pass absorption [28]. This approach employs a mirror to reflect the residual pump source back into the crystal, thereby promoting re-absorption of the residual pump and improving the pump energy storage efficiency. The four-pass absorption rate of the pump light stands at 98.9% (red solid line in Figure 2(d)). After four-pass absorption, the residual pump accounts for roughly 1% (posing no risk to the array of LD), and the pump efficiency experiences an improvement of about 10.1% compared to the twice absorption. It should be noted that all subsequent experiments in this work are carried out under the operating condition where the crystal absorbs the pump source twice.

Downloaded from https://www.cambridge.org/core. 17 Nov 2026 at 18:24:11, subject to the Cambridge Core terms of use.

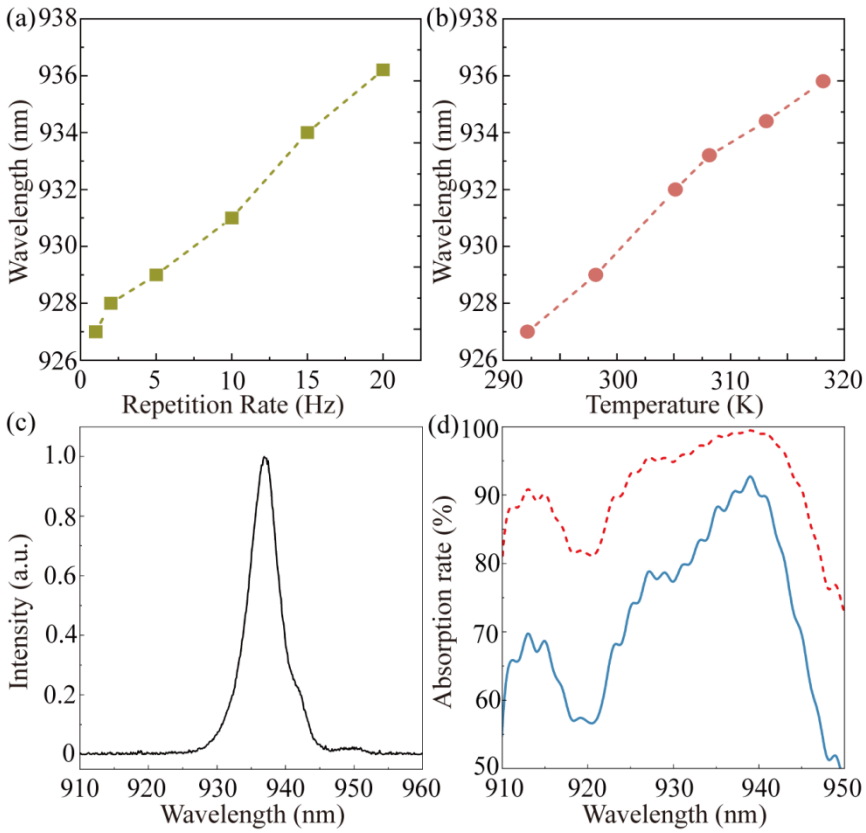


Figure 2. (a) Output central wavelength of the LD as a function of repetition rate at 292.15 K. (b) Output central wavelength of the LD as a function of cooling-water temperature at 1 Hz. (c) Measured output spectrum of the LD by a Spectrometer (Ocean Optics, HR-4N1000-5) at 1 Hz and 318.15 K. (d) Calculated absorption rate in Yb:YAG crystal of the LD with two-pass (four-pass) absorption represented by cyan solid (red dashed) line. The output spectrum shown in (c) was considered in the calculations.

III. Experimental amplification results

3.1 Gain experiment

Prior to system description, we studied on the gain capability of the active mirror amplifier, demonstrating the potential of room-temperature Yb:YAG amplifiers. We first tested the output power of LD as a function of input current at 1 Hz, achieving a maximum output power of about 100 kW@400 A (Figure 3(a)). Note: the output power is theoretically influenced by junction temperature, increasing as the temperature decreases. Nevertheless, the effect is negligible due to the increment merely exceeding the measurement error, and thus is hard to observe in practice. The pump area suffers an attenuation of roughly 8% when traveling through glass and cooling water, which has dimensions of 36×16 mm^2, corresponding to a pump intensity of ~16 kW/cm^2.

Downloaded from https://www.cambridge.org/core. 17 Nov 2026 at 18:24:11, subject to the Cambridge Core terms of use.

Next, we investigated the relationship between pump pulse duration and gain coefficient. The gain coefficient is defined as the gain obtained when the seed laser is incident on the gain medium from the front surface at the Brewster angle, reflected by high-reflective coating on the rear surface, and exited the gain medium again through the front surface. The fluorescence lifetime of Yb:YAG is 940 μs, and a suitable increase in pump pulse duration can enhance the gain coefficient. Employing a single gain medium and its corresponding LD array, with a pump current of 400 A, a repetition rate of 1 Hz, a cooling-water temperature of 308.15 K, we progressively extended the pump pulse duration from 0.9 ms to 1.2 ms. The maximum gain coefficient can reach 2.64 at 1.2 ms, as shown in Figure 3(b). For each 100-μs increase in pulse duration, the gain has an approximate 10% increase. To avoid unduly shortening the lifetime of LD and promise an adequate gain, the pump pulse duration was fixed at 1.2 ms for subsequent experiments.

The gain coefficient was then evaluated as a function of the LD cooling-water temperature at a pump pulse duration of 1.2 ms and a repetition rate of 1 Hz. As the cooling-water temperature gradually rose, the gain coefficient slowly climbed, ranging from 2.56 at 298.15 K to 2.75 at 318.15 K (Figure 3(c)). This increase correlates with a redshift of the LD emission wavelength at elevated temperatures. Specifically, a 20-K rise in water temperature leads to less than a 10% increase of the gain coefficient, but this improvement comes at the expense of reducing the lifetime of LD. The slight improvement may appear unreasonable: the LD output wavelengths at temperatures of 298.15 K and 318.15 K are 929.0 nm and 935.8 nm (Figure 2(b)), respectively. This behavior is attributed to the fact that when the stored energy is sufficient, the gain coefficient becomes less sensitive to the exact central wavelength of pump.

We finally explored the dependence on the gain coefficient and repetition rate of the seed pulse, with a pump pulse duration of 1.2 ms and an LD cooling-water temperature set at 308.15 K. Gain coefficients of 2.64, 2.53, 2.50, and 1.91 were obtained in sequence at repetition rates of 1, 2, 5, and 10 Hz, respectively (Figure 3(d)). When the pump current exceeds 350 A, an increase in the repetition rate induces a more pronounced temperature rise in the gain medium, accompanied by a redshift of the LD output wavelength. The impact of the gain medium temperature rise on gain coefficient dominates over that of the redshift in the LD output wavelength. Therefore, under high-intensity pumping, the highest gain is achieved at a repetition rate of 1 Hz.

Downloaded from https://www.cambridge.org/core. 17 Nov 2026 at 18:24:11, subject to the Cambridge Core terms of use.

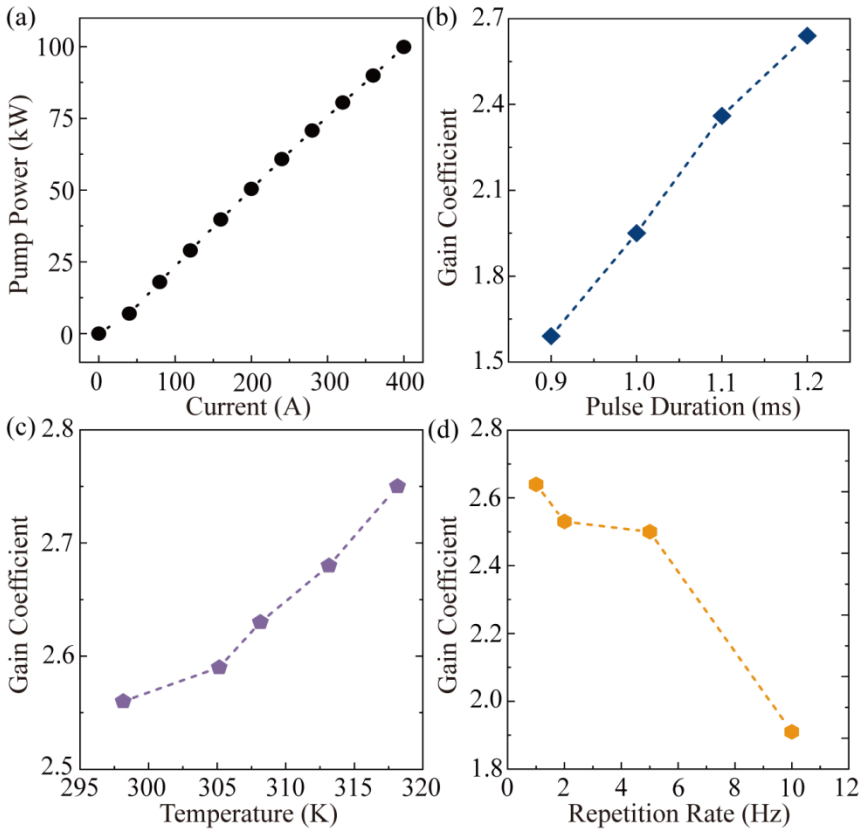


Figure 3. (a) Pulse power of the pump as a function of input current at 1 Hz. (b) The gain coefficient as a function of pulse duration at 1 Hz and 308.15 K. (c) The gain coefficient as a function of cooling-water temperature at 1 Hz and 1.2 ms. (d) The gain coefficient as a function of repetition rate at 1.2 ms and 308.15 K.

3.2 Performance of 3-J compact system

Based on the above characteristics of room-temperature active mirror amplifier, we have developed a compact system delivering 3-J pulses with an FWHM duration of 10 ns. The whole system is schematically shown in Figure 4, which makes full use of our home-built advanced lasers: the maximum output power was about 350 mJ, and the pulse duration was 10 ns. Unfortunately, the repetition frequency was fixed at 1 Hz. The output pulses were intrinsically time-synchronized with pump source via a signal synchronizer. Subsequent experiments reported in this paper are performed using this home-built seed laser.

Downloaded from https://www.cambridge.org/core. 17 Nov 2026 at 18:24:11, subject to the Cambridge Core terms of use.

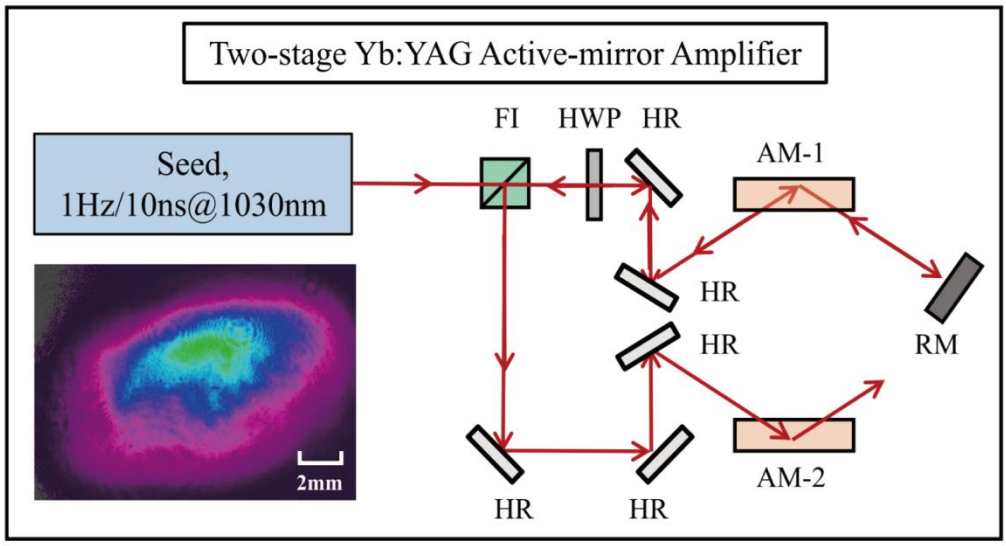


Figure 4. Schematic diagram of two-stage Yb:YAG-based active-mirror amplifier system at 293 K. FI: Faraday isolator; HWP: half-wave plate; HR: high-reflection mirror; RM: return mirror; AM: active mirror. Inset: the seed beam profile with an energy of 300 mJ.

The single-pass absorption rate of signal in crystal is ~55.0%, while that of the pump is ~89%. Yb:YAG, which serves as both a beam combiner and a reflecting mirror, requires strict injection at the Brewster angle due to the sensitivity of its transmission to the input angle and polarization. Figure 5 shows the output energy for seeded energy of 110 mJ (a), 207 mJ (b), and 302 mJ (c). In all three cases, the injected signal energy is less than 1% of the stored pump energy. The general trend of the amplified signal output as a function of pump current remains consistent. The single-pass amplification can be considered as a small-signal gain. The gain coefficients are essentially 2.50, as shown in Figure 5(d). In this regime, the spatial overlap between the signal and the pump is not critical, owing to the sufficient pump energy available.

Downloaded from https://www.cambridge.org/core. 17 Nov 2026 at 18:24:11, subject to the Cambridge Core terms of use.

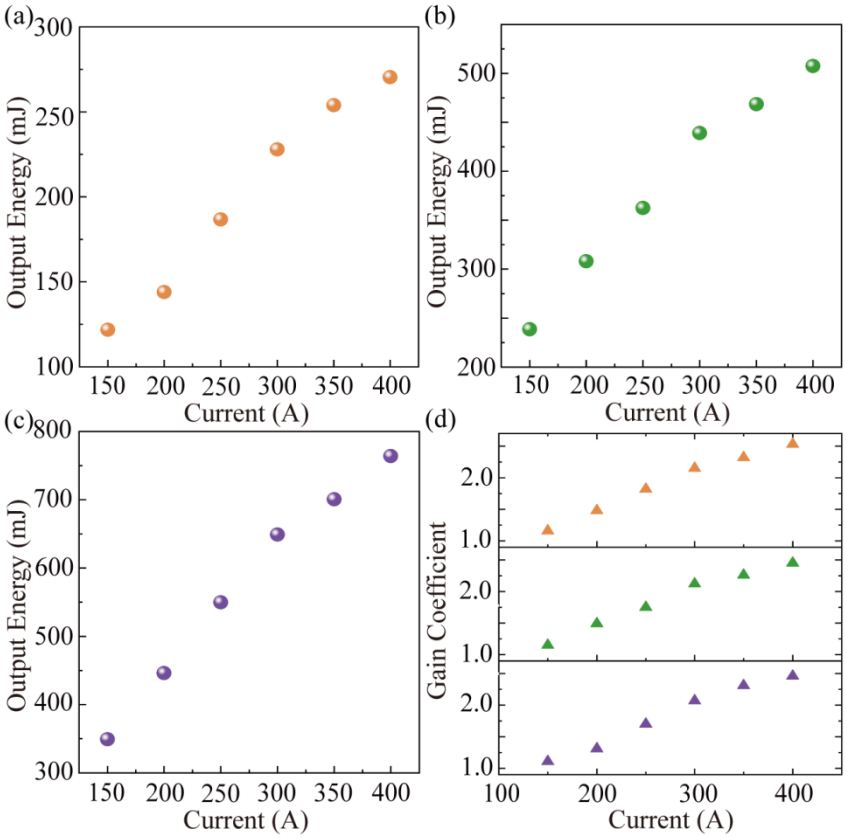


Figure 5. Output energy of single-pass Yb:YAG-based active mirror in the first stage as a function of pump current. The orange, green and purple dots represent different seeded energy. The seeded energy of (a), (b), and (c) is 110, 207, and 302 mJ, respectively. (d) The gain coefficient of different seeded energy as a function of pump current.

Subsequently, we studied a double-pass amplifier in the first-stage for achieving a larger amplification. Maintaining the same injection as those in Figure 5, the output curves of the first-stage double-pass amplifier are illustrated in Figure 6 (a), (b), and (c). In contrast to single-pass amplification where the gain coefficient (~2.5) remains insensitive to injected energy, the double-pass amplifier exhibits a clear dependence. With seeded energies of 100, 200, and 300 mJ, and a pump current of 400 A, the output energies reach 6.13, 5.29, and 5.07 times that of the input. The theoretical gain coefficient for double-pass amplification calculated to be 6.25. This observed decrease arises from pump depletion. Furthermore, a higher gain coefficient can be achieved by increasing the number of extraction passes.

Downloaded from https://www.cambridge.org/core. 17 Nov 2026 at 18:24:11, subject to the Cambridge Core terms of use.

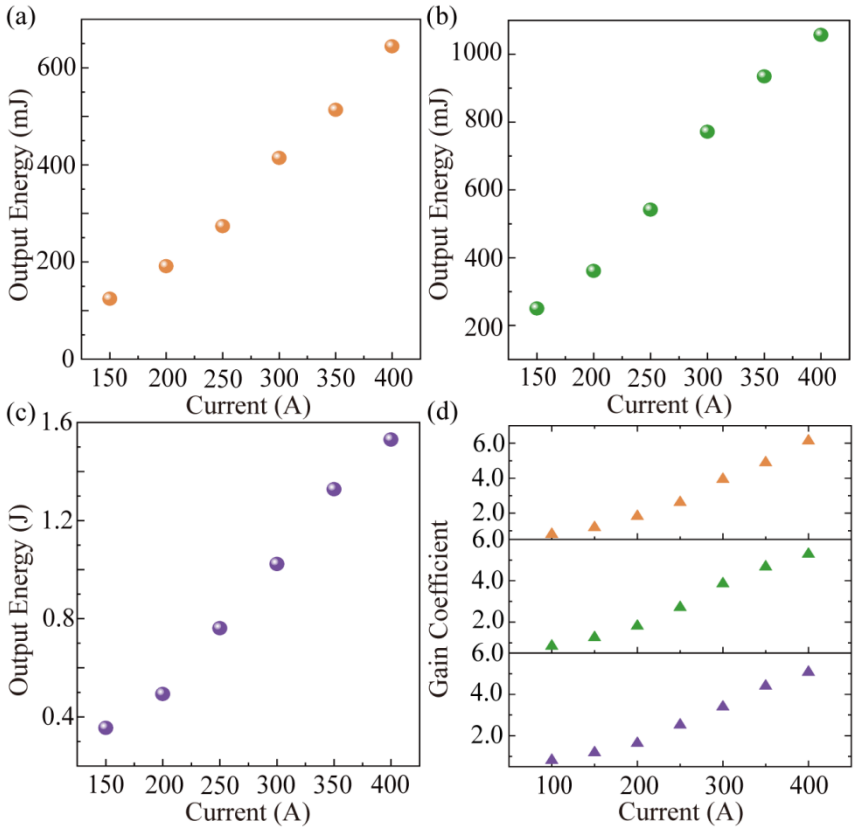


Figure 6. Output energy of two-pass Yb:YAG-based active mirror in the first stage as a function of pump current. The orange, green and purple dots represent different seeded energy. The seeded energy of (a), (b), and (c) is 110, 207, and 302 mJ, respectively. (d) The gain coefficient of different seeded energy as a function of pump current.

To maximize the final output of the two-stage active mirror amplifier, we adopted a configuration combining a double-pass first stage with a single-pass second stage. Both stages share an identical pump source. The pulse from the first-stage amplifier, after passing through a Faraday isolator and reflective mirrors, possessed an energy of 1.2 J at the front surface of gain medium in the second-stage. We achieved an output of ~3 J/1 Hz/10 ns with a pump current of 400 A (purple dots shown in Figure 7). A gain coefficient of 2.5 is maintained, which is attributed to the high saturation fluence (~9.6 J/cm^2) of Yb:YAG, indicating that higher energy output can be realized by increasing the injection fluence.

Downloaded from https://www.cambridge.org/core. 17 Nov 2026 at 18:24:11, subject to the Cambridge Core terms of use.

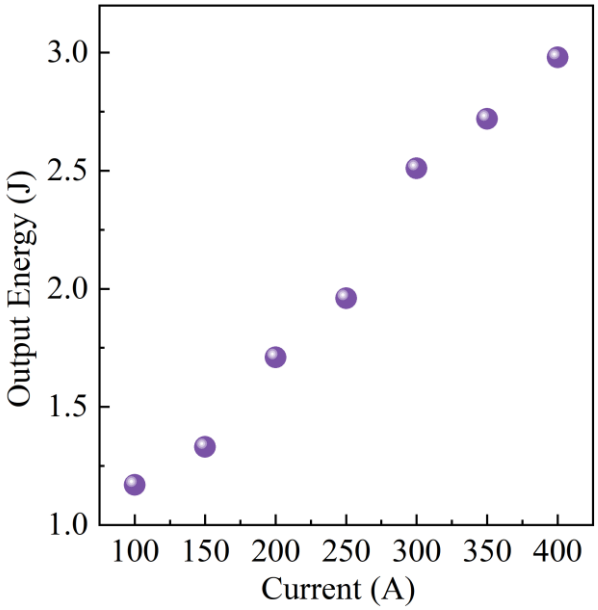


Figure 7. Output energy of a single pass at the second stage laser amplifier as a function of pump current, seeding an effective pulse energy of ~1.2 J.

Finally, we demonstrated the output beam quality of the system. Figure 8 shows the measured output beam profiles at a pulse energy of 3 J and a repetition rate of 1 Hz. An average beam size of ~8×12 mm^2 (full width at 1/e^2 maximum) was measured at a position 0.5 m behind the second amplifier. Due to the relatively poor near- and far-field beam quality of the injected 300 mJ seed (inset in Figure 4), we could only compare the near-field beam profiles in horizontal and vertical directions before and after amplification. After amplification, the near-field beam profile fidelity exceeded 96% in both directions, indicating excellent preservation of the beam shape. In future work, we aim to improve the quality of the 300 mJ injection and conduct more comprehensive quantitative characterization.The small sharp features were attributed to dust on filters used in the front of the beam profiler. The mean fluence is 3.98 J/cm^2, which suggests a maximum value of 7.10 J/cm^2 according to Ref. [15]. The damage threshold of the high- or anti-reflection coating is 15 J/cm^2 at 10 ns/10 Hz/1030 nm. The output energy fluctuation (shown in Figure 9) was measured over 300 shots at the highest energy (~3 J). Futhermore, we can improve the temporal waveform, and energy stability of the seed source to improve the output stability. Since the peak fluence of the maximum energy is approximately half of the damage threshold, the system can operate without accident.

Downloaded from https://www.cambridge.org/core. 17 Nov 2026 at 18:24:11, subject to the Cambridge Core terms of use.

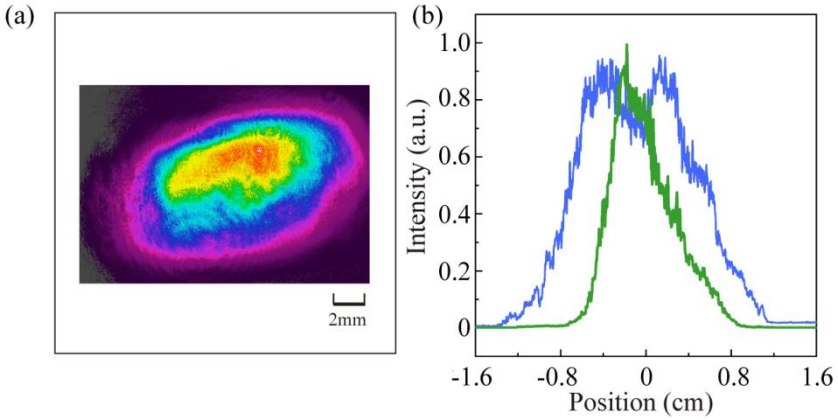


Figure 8. (a) Output beam profile of near field at a 3 J pulse energy of the laser amplifier. The small sharp features are due to the dust on the used filters in front of the camera. (b) The horizontal (blue) and vertical (green) profile versus position of near field.

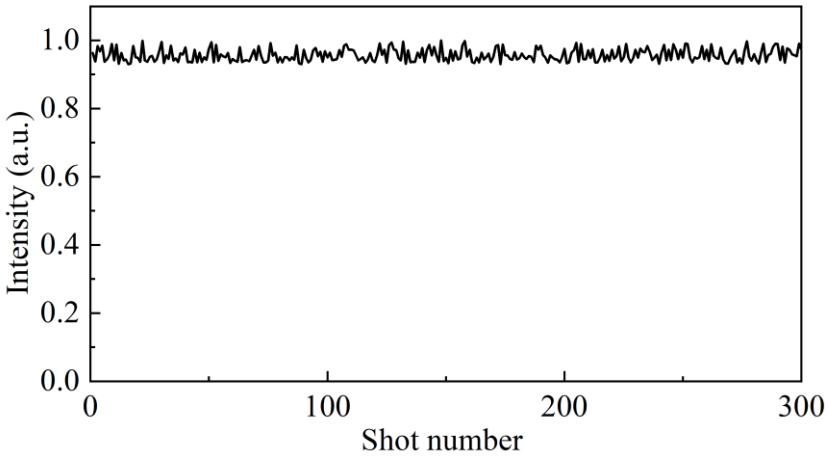


Figure 9. Relative trend of amplified pulse energy within 300 shots at the highest energy (~3 J).

IV. Conclusion

In summary, we have experimentally demonstrated a large-aperture active mirror amplifier operating at room temperature. A carefully designed packaging and coating scheme for the active mirror amplifier was developed. Furthermore, we have studied gain experiments on this amplifier under various operating conditions, including different repetition rate, pump pulse duration, and cooling-water temperature. With a seed energy of 300 mJ, we have successfully achieved an output of 3 J at a repetition rate of 1 Hz. The Yb:YAG-based active mirror amplifier stands out for its compact structure and high pump storage efficiency, offering the potential for tabletop-scale ×10 J output. These results hold significant promise for extending the practical application of high-energy lasers beyond the laboratory into a wider array of scenarios.

Downloaded from https://www.cambridge.org/core. 17 Nov 2026 at 18:24:11, subject to the Cambridge Core terms of use.

Acknowledgements

This work was supported by National Natural Science Foundation of China (62405298, 62305318), the President Funding Independent Project of China Academy of Engineering Physics (YZJJZL2024200) and National Key Research and Development Program (2023YFA1608503). The authors thank Kui Yi from Shanghai Institute of Optics and Fine Mechanics, Chinese Academy of Sciences, for the discussion about high-quality coating of Yb:YAG crystals.

References

1. J. Lu, M. Prabhu, J. Song, C. Li, J. Xu, K. Ueda, A. A. Kaminskii, H. Yagi, T. Yanagitani, "Optical properties and highly efficient laser oscillation of Nd:YAG ceramics", Appl. Phys. B **71**(4): 469-473 (2000). DOI: https://doi.org/10.1007/s003400000394
2. T. Y. Fan, "Heat generation in Nd: YAG and Yb:YAG", IEEE J. Quantum Electron. **29**(6): 1457-1459 (1993). DOI: https://doi.org/10.1109/3.234394
3. J. Shang, J. Wang, W. Peng, H. Liu, D. Wang, Y. Ma, B. Fu, Y. Yu, Y. Feng, L. Zhang, X. Ruan, Q. Jin, J. Yi, X. Ye, Y. Sun, W. Wang, Q. Gao, "Research progress and prospects of laser diode pumped high-energy laser", High Power Laser Part. Beams **34**(1): 011007 (2022). DOI: https://doi.org/10.11884/HPLPB202234.210530
4. H. Yu, W. Duan, M. Xu, X. Jiang, "Review of Ytterbium-Doped Laser Materials", Laser Optoelectron. Prog. **44**(5): 30-41 (2007).
5. J. G. Zheng, X. Y. Jiang, X. W. Yan, J. Zhang, Z. G. Wang, D. S. Wu, X. L. Tian, X. J. Zhang, M. Z. Li, Q. H. Zhu, J. Q. Su, F. Jing, and W. G. Zheng, "Progress of the 10 J water-cooled Yb:YAG laser system in RCLF", High Power Laser Sci. Eng. **2**, e27 (2014). DOI: https://doi.org/10.1017/hpl.2014.29
6. A. Yoshida, S. Tokita, J. Kawanaka, T. Yanagitani, H. Yagi, F. Yamamura, and T. J. Kawashima, "Numerical laser gain estimation of cryogenic Yb:YAG ceramics for IFE reactor driver", Phys. Conf. Ser. **112**(3): 032062 (2008). DOI: https://doi.org/10.1088/1742-6596/112/3/032062

Downloaded from https://www.cambridge.org/core. 17 Nov 2026 at 18:24:11, subject to the Cambridge Core terms of use.

7. C. Hönninger, I. Johannsen, M. Moser, G. Zhang, A. Giesen, U. Keller, “Diode-pumped thin-disk Yb:YAG regenerative amplifier”, Appl. Phys. B **65**: 423-426 (1997). DOI: https://doi.org/10.1007/s003400050291
8. W. Huang, J. Wang, X. Lu, and X. Li, “A highly stable laser diode pumped cryogenic Yb:YAG nanosecond regenerative amplifier”, Laser Phys. **23**(3): 035804 (2013). DOI: https://doi.org/10.1088/1054-660X/23/3/035804
9. I. B. Mukhin, O. V. Palashov, E. A. Khazanov, A. Ikesue, and Y. L. Aung, “Experimental study of thermally induced depolarization in Nd:YAG ceramics”, Opt. Express **13**(16): 5983-5987 (2005). DOI: https://doi.org/10.1364/OPEX.13.005983
10. H Yoshioka, S Nakamura, T Ogawa, S Wada, “Diode-pumped mode-locked Yb: YAG ceramic laser”, Opt. Express **17**(11): 8919-8925 (2009). DOI: https://doi.org/10.1364/OE.17.008919
11. C. Wandt, S. Klingebiel, M. Siebold, Z. Major, J. Hein, F. Krausz, and S. Karsch, “Generation of nanosecond pulses at a repetition rate with excellent beam quality in a diode-pumped Yb:YAG MOPA system”, Opt. Lett. **33**(10): 1111-1113 (2008). DOI: https://doi.org/10.1364/OL.33.001111
12. J. Tümmler, R. Jung, H. Stiel, P. V. Nickles, and W. Sandner, “High-repetition-rate chirped-pulse-amplification thin-disk laser system with joule-level pulse energy”, Opt. Lett. **34**(9): 1378-1380 (2009). DOI: https://doi.org/10.1364/OL.34.001378
13. S. Klingebiel, C. Wandt, C. Skrobol, I. Ahmad, S. A. Trushin, Z. Major, F. Krausz, and S. Karsch, “High energy picosecond Yb:YAG CPA system at 10 Hz repetition rate for pumping optical parametric amplifiers”, Optics Express **19**(6): 5357-5363 (2011). DOI: https://doi.org/10.1364/OE.19.005357
14. M. Chyla, M. Smrz, T. Mocek, “High-energy, picosecond regenerative thin-disk amplifier at 1 kHz”, Solid State Lasers XXI: Technology and Devices **8235**: 400-406 (2012). DOI: https://doi.org/10.1117/12.908150
15. C. Wandt, S. Klingebiel, S. Keppler, M. Hornung, M. Loeser, M. Siebold, C. Skrobol, A. Kessel, S. A. Trushin, Z. Major, J. Hein, M. C. Kaluza, F. Krausz, S. Karsch, “Development of a Joule-class Yb:YAG amplifier and its implementation in a CPA system generating 1 TW pulses”, Laser Photonics Rev. **8**(6): 875-881 (2014). DOI: https://doi.org/10.1002/lpor.201400040

Downloaded from https://www.cambridge.org/core. 17 Nov 2026 at 18:24:11, subject to the Cambridge Core terms of use.

16. S. Klingebiel, M. Schultze, C. Y. Teisset, R. Bessing, M. Häfner, S. Prinz, M. Gorjan, D. Sutter, K. Michel, H. G. Barros, Z. Major, F. Krausz, and T. Metzger, "220 mJ ultrafast thin-disk regenerative amplifier", CLEO: 2015, OSA Technical Digest (online) (Optica Publishing Group, 2015) paper STu4O.2. DOI: https://doi.org/10.1364/CLEO_SI.2015.STu4O.2
17. R. Jung, J. Tümmler, and I. Will, "Regenerative thin-disk amplifier for 300 mJ pulse energy", Opt. Express **24**(2): 883-887 (2016). DOI: https://doi.org/10.1364/OE.24.000883
18. R. Jung, J. Tümmler, T. Nubbemeyer, and I. Will, "Thin-disk ring amplifier for high pulse energy", Opt. Express **24**(5): 4375-4381 (2016). DOI: https://doi.org/10.1364/OE.24.004375
19. T. Nubbemeyer, M. Kaumanns, M. Ueffing, M. Gorjan, A. Alismail, H. Fattahi, J. Brons, O. Pronin, H. G. Barros, Z. Major, T. Metzger, D. Sutter, and F. Krausz, "1 kW, 200 mJ picosecond thin-disk laser system", Opt. Lett. **42**(7): 1381-1384 (2017). DOI: https://doi.org/10.1364/OL.42.001381
20. C. Herkommer, P. Krötz, R. Jung, S. Klingebiel, C. Wandt, R. Bessing, P. Walch, T. Produit, K. Michel, D. Bauer, R. Kienberger, and T. Metzger, "Ultrafast thin-disk multipass amplifier with 720 mJ operating at kilohertz repetition rate for applications in atmospheric research", Opt. Express **28**(20): 30164-30173 (2020). DOI: https://doi.org/10.1364/OE.404185
21. Y. Chen, J. Yu, Z. Yao, X. Zhang, J. Sun, Y. Zhang, F. Chen, "Thin-disk regenerative amplifier with 110 mJ, 2.1 ps, 1kHz repetition rate laser output", Chin. J. Lasers **51**(13): 1315001 (2024). DOI: https://doi.org/10.3788/CJL240532
22. J. C. Chanteloup, H. Yu, G. Bourdet, C. Dambrine, S. Ferré, A. Fülöp, S. L. Moal, A. Pichot, G. L. Touzé and Z. Zhao, "Overview of the Lucia laser program: towards 100 Joules, nanosecond pulses, kW averaged power, based on Ytterbium Diode Pumped Solid State Laser", Solid State Lasers XIV: Technology and Devices. SPIE **5707**: 105-116 (2005). DOI: https://doi.org/10.1117/12.588341
23. D. Albach, J. C. Chanteloup, G. L. Touzé, "Influence of ASE on the gain distribution in large size, high gain Yb^{3+}:YAG slabs", Opt. Express **17**(5): 3792-3801 (2009). DOI: https://doi.org/10.1364/OE.17.003792
24. D. Albach, M. Arzakantsyan, G. Bourdet, J. C. Chanteloup, P. Hollander, and B. Vincent, "Current status of the LUCIA laser system", Journal of Physics: Conference Series **244**(3): 032015 (2010). DOI: https://doi.org/10.1088/1742-6596/244/3/032015

Downloaded from https://www.cambridge.org/core. 17 Nov 2026 at 18:24:11, subject to the Cambridge Core terms of use.

25. T. Gonçalvès-Novo, D. Albach, B. Vincent, M. Arzakantsyan, and J. Chanteloup, “14 J/2 Hz Yb^{3+}:YAG diode pumped solid state laser chain”, Opt. Express **21**(1): 855-866 (2013). DOI: https://doi.org/10.1364/OE.21.000855
26. J. Liu, X. Guan, L. Ji, T. Wang, F. Zhang, J. Liu, Z. Sui, Y. Cui, X. Zhao, Y. Gao, “Optical Scheme Simulation of Table-Top 20 TW Laser Based on Yb:YGG”, Acta Opt. Sin. **44**(20): 2014006 (2024). DOI: https://doi.org/10.3788/AOS240868
27. X. Guan, Z. Sui, Y. Gao, Y. Cui, L. Ji, F. Zhang, J. Liu, “A compact laser amplification system and method based on spatial multiplexing structure”, China patent CN116979355A (October 31, 2023).
28. J. Liu, J. Lai, Y. Cui, X. Zhao, Z. Sui, Y. Gao, “A pump coupling system”, China patent CN122225267A (June 16, 2026).s

Downloaded from https://www.cambridge.org/core. 17 Nov 2026 at 18:24:11, subject to the Cambridge Core terms of use.